Transactions of KSAE, Vol. 33, No. 8, pp.673-686 (August, 2025)

Check for updates

Copyright © 2025 KSAE / 237-10
pISSN 1225-6382 / eISSN 2234-0149
DOI http://dx.doi.org/10.7467/KSAE.2025.33.8.673

Research on Gear Ratios Selection Considering Drive Motor Efficiency and Battery SOC Changes

Kol Bambag Phinees · Hyeon-Seop Yi*

Department of Mechanical Engineering, SunMoon University, Chungnam 31460, Korea

(Received 4 March 2025 / Revised 10 June 2025 / Accepted 19 June 2025)

Abstract : In electric vehicles(EVs), metrics such as motor efficiency and battery State of Charge(SOC) are critical in assessing overall performance because they serve a similar function to fuel efficiency in internal combustion engine vehicles. Optimizing the transmission system's reduction ratio and gear ratio is crucial to improving power transmission efficiency and sustaining battery SOC. This paper introduces the concept of employing a multi-speed transmission system to optimize EV performance across different driving cycles and enhance energy efficiency, acceleration, and overall drivability. An EV advance simulator equipped with a reduction gear is developed by selecting suitable multi-speed transmission candidates based on the efficiency curve of the drive motor. The optimal gear ratio is determined through virtual driving simulations using a dynamic programming approach, which incorporates a cost function to optimize energy efficiency and driving performance.

Key words : Electric vehicle, Multi-speed transmission, Reduction ratio, Gear ratio optimization, Vehicle performances, Powertrain

Nomenclature

A : vehicle frontal area, m^2
a_{req} : vehicle longitudinal acceleration, m/s^2
C_d : air resistance coefficient
F_{roll} : rolling resistance force, N
F_{aeroDy} : aerodynamic drag force, N
F_{Climb} : climbing resistance force, N
F_{ac} : acceleration resistance force, N
F_{TF} : traction force, N
F_x : traction force at the tire ground contact, N
f_r : rolling resistance coefficient
g : acceleration of gravity, m/s^2
I_d : rotational inertia of the drive system, kg · m^2
I_w : rotational inertia of wheel and axle, kg · m^2
I_t : rotational inertia of the transmission, kg · m^2
I_{bat} : current of the battery, A
I_e : motor rotational inertia, kg · m^2
m : vehicle mass, kg
N_f : final drive ratio
N_t : transmission gear numerical ratio
P_{bat} : battery power, W
Q_{bat} : nominal capacity of the battery, A · h
$R(soc)$: internal resistance of the battery, ohm
r_i : gear ratio candidate
r_{i_min} : minimum gear ratio candidate
r_{i_max} : maximum gear ratio candidate
r : tire radius, m
$\dot{soc}$: varying of the battery state-of-charge, %
T_a : traction acting on the axle, N · m
T_d : driving torque demand, N · m
T_b : braking torque demand, N · m
T_e : motor torque, N · m
T_c : input torque from the motor acceleration, N · m
T_{e_max} : maximum motor torque. N · m
T_{b_max} : maximum brake torque, N · m
V_{veh} : vehicle speed, m/s
$V(soc)$: open circuit voltage of the battery, V
α_w : angular acceleration of wheel, rad/s^2

*Corresponding author, E-mail: hyeonseop840@sunmoon.ackr

α_d : angular acceleratio drive system, rad/s^2
α_e : motor angular accelartion, rad/s^2
ρ : air density, kg/m^3
$\eta_{drivetrain}$: drivetrain efficiency, percentage
η_{motor} : motor efficiency, percentage
η_{total} : total efficiency, percentage

Subscripts

DC : drive command
EV : electric vehicle
SOC : state-of-charge

1. Introduction

In today's world, emissions from combustion-engine vehicles are significant contributors to rising global temperatures and unpredictable climate changes. These environmental challenges have accelerated the automobile industry's shift toward the production of electric vehicles as a sustainable alternative, which is a crucial step toward fostering a zero-emission future.[1] The powertrain system, which includes the electric motor, battery, and transmission, is central to the performance and efficiency of EVs. Among these components, the selection of gear ratios is an important factor in sharping the vehicle's overall efficiency, driving range, and dynamic performance.[2] However, optimizing gear ratios in EVs is a complex task, as it requires balancing multiple interdependent factors, including the operating efficiency of the electric motor and the dynamic changes in the battery's state of charge(SOC).[3] Electric motors exhibit varying efficiency levels depending on their operating points, which are influenced by speed and torque demands.[4] Unlike internal combustion engines, electric motors have distinct efficiency maps with high-efficiency regions that must be leveraged to minimize energy losses.[5] The gear ratio directly affects the motor's operating point by translating vehicle speed and torque requirements into motor speed and torque.[6] An improperly selected gear ratio can force the motor to operate outside its optimal efficiency range, leading to increased energy consumption and reduced driving range.[7] Furthermore, the battery's SOC, which reflects the available energy, is highly sensitive to the power demands placed on it.[8] The gear ratio, by modulating the torque and speed relationship between the motor and the wheels, can influence the power demand profile and, consequently, the rate of SOC change.[9] Therefore, an optimal gear ratio must maximize motor efficiency and ensure that the battery operates within a stable SOC range to prolong its lifespan and maintain consistent performance.[10] Despite the critical importance of gear ratio selection, existing research often treats motor efficiency and battery SOC as separate considerations, neglecting their interconnected effects on vehicle performance.[11] Previous motor-centric studies focused exclusively on optimizing gear ratios based on motor efficiency maps,[3,6] while battery-oriented research examined SOC dynamics without considering transmission design opportunities.[6,8] This gap in the literature underscores the need for a holistic approach that integrates both factors into the gear ratio optimization process. Recent attempts to bridge this divide have made progress through adaptive control methods, but remain limited by their neglect of mechanical constraints and interactions between components, and their reliance on idealized driving cycles.[10] By doing so, it becomes possible to achieve a synergistic balance that enhances overall system efficiency, extends driving range, and ensures reliable battery operation.[12]

This research addresses this challenge by developing a comprehensive methodology for gear ratio selection that simultaneously considers drive motor efficiency and battery SOC dynamics under varied drive cycles. Through detailed system modeling and simulation-based validation, this study aims to identify gear ratios for multi-speed transmissions that optimize the trade-offs between motor efficiency, battery SOC changes, and vehicle performance. The remainder of this study is outlined as follows. Part 2 describes the EV's system modeling approach, including motor efficiency maps, battery models, and vehicle dynamics. Part 3 shows the validation model of the simulation. Part 4 provides the optimization framework to determine the optimal gear ratio of each stage during the selection process. Part 5 discusses the simulation results and their implications. Finally, Part 6 concludes the paper with key findings.

2. System Modeling and Dynamics Description

To ensure the accuracy of the study findings, a simulated commercial EV model with a shift pattern was developed based on real vehicle specifications to provide optimal

dynamics and economic performance.

2.1 Vehicle Longitudinal Control

In this section, the vehicle's longitudinal power transmission system, which comprises the battery, control unit, electric motor, reducer, final drive, and wheels, generates and transmits rotational energy. To facilitate the selection of the optimal gear ratio for a multi-speed transmission, a longitudinal powertrain simulator was developed within a MATLAB/Simulink environment for the conventional electric vehicle under study, as shown in Fig. 1. This simulator accurately models the vehicle's longitudinal control, providing insights into the interaction of various components and their impact on overall performance in the selection of the optimal gear ratio based on the specifications of the EV listed in Table 1.

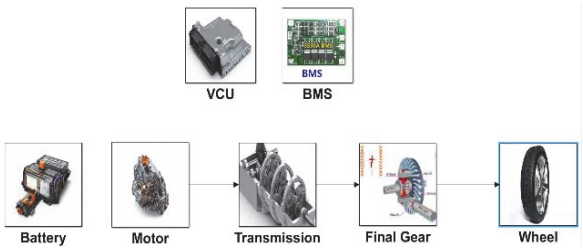

Fig. 1 Powertrain connection of the electric vehicle

Table 1 Vehicle specification reference

General data	
Mass[kg]	2,000
Gravity	9.81
Aero data	
Drag coefficient	0.52
Downforce coefficient	1.2
Front area [m^2]	2.5
Air density [kg/m^2]	1.226
Tire data	
Tire radius[m]	0.34
Rolling friction	0.015
Longitudinal friction	1.4
Lateral friction	1.5
Transmission	
Final drive ratio	3.9
Powertrain efficiency [%]	0.95

2.2 Vehicle Longitudinal Dynamics

Vehicle longitudinal dynamics describe the forces and motions along the direction of travel, which are crucial for accurately simulating and controlling vehicle behavior. A predictive model provides a mathematical framework to estimate these dynamics, enabling better powertrain control and energy management.

The predictive model intergrates several factors and the driving forces developed by the motor that overcome the climbing resistance F_{Climb}, aerodynamic drag F_{aeroDy}, rolling resistance F_{roll}, and acceleration F_{ac}, given by the following equation.[13)]

$$F_{TF} = F_{roll} + F_{aeroDy} + F_{Climb} + F_{ac}(N) \tag{1}$$

Where the traditional binomial representation of the resistant load due to the aerodynamic, rolling, climbing and acceleration resistance is expressed as follows:

$$F_{TF} = f_r.mgcos\theta + 0.5\rho C_d A V_{veh}^2 + mgsin\theta + ma_{req} \tag{2}$$

The following Eq. (3) describes the tire load used in the simulation to calculate the forces and torques acting on the tire and axle, considering the rotational inertia of the wheel and the traction force generated at the tire-ground contact.

$$T_a = F_x r + I_w \times \alpha_w = (T_d - I_d \times a_d) N_f \tag{3}$$

Where T_a represents the torque acting on the axle, r the tire radius, F_x traction force at the tire ground contact, I_w rotational inertia of the wheel and axle, a_w angular acceleration of the wheel, a_d acceleration of the drive system, I_d rotational inertia of the drive system, and N_t the final drive gear ratio.

2.2.1 Electric Motor and Transmission Model

Based on Table 2, the electric motor model was developed for simulation with the MATLAB/Simulink program to reflect the motor torque speed and efficiency map, as shown in Fig. 2. The torque-speed characteristics and efficiency contour allow to identify the operating points that offer the highest efficiency during the simulation.

The following equation gives the transmission model used in this simulation:[14)]

Table 2 Motor parameters

Parameter	Value
Max torque [N · m]	353
Max speed [RPM]	8,000
Maximum efficiency [%]	95

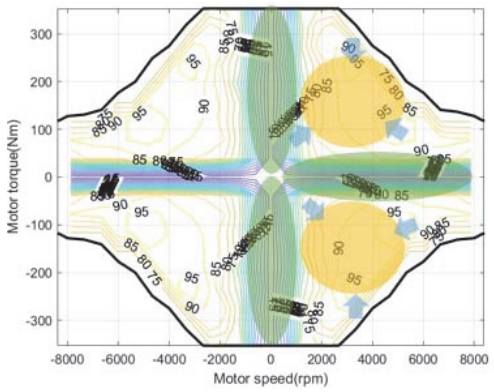

Fig. 2 Motor efficiency map

$$T_c = T_e - I_e \alpha_e \tag{4}$$

Eq. (4) describes the torque transmitted through the motor acceleration as a transmission input torque, where T_e is the motor torque, I_e the motor rotational inertia, and α_e the motor angular acceleration.

$$T_d = (T_c - I_t \alpha_e) N_t \tag{5}$$

Eq. (5) describes output torque transmission magnified by the gear ratio of the transmission and reduced by the inertial losses of the gears and axles. Where T_d is the output torque from the transmission T_c is the input torque from the motor's angular acceleration, I_t the rotational inertia of the transmission, and α_e the motor acceleration.

2.2.2 Battery

The type of battery adopted was a lithium-ion type, as listed in Table 3. Therefore, for the simulation, the battery is modeled as an equivalent circuit using the internal resistance model, where the open circuit voltage and internal resistance are treated as functions to estimate the battery's state-of-charge (SOC) consumption after driving. This battery model allows us to consider the charging-discharging characteristics during driving, as shown in Fig. 3 and Fig. 4. The SOC consumption equation is described as follows.[16)]

$$\dot{soc} = \frac{\mathrm{V}(soc) - \sqrt{\mathrm{V}(soc)^2 - 4.R(soc).P_{bat}}}{2.R(soc).Q_{bat}} \tag{6}$$

Where $\dot{soc}$ denotes the varying of the battery SOC and Q_{bat} denotes the battery's nominal capacity.

$$P_{bat} = V(soc).I_{bat} - I_{bat}^2.R(soc) \tag{7}$$

Eq. (6) describes the relationship between the battery power, V(soc), the open circuit voltage, R(soc), the internal resistance, and the battery's current.

Table 3 Battery parameters

Battery li-ion-300	
Capacity [A.h]	285
Power max [W]	297,096
Rated Voltage [V]	355

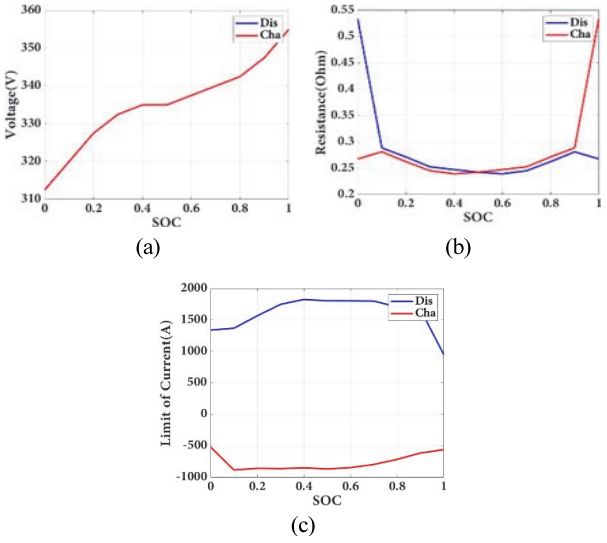

Fig. 3 (a) Internal voltage, (b) Internal resistance, (c) Internal limit current

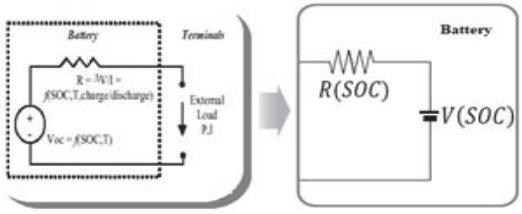

Fig. 4 Equivalent circuit of battery model

2.2.3 Electric Vehicle Control unit Model

The VCU model can integrate brake torque to maximize drivability and regenerative energy in braking mode and generate the driving torque demand in driving mode, thereby improving the EV's battery state-of-charge(SOC). Where the driving torque demand T_d is given by

$$T_d = T_{e\_max}(\alpha_e)DC \tag{8}$$

And the braking torque demand is given by

$$T_b = T_{b\_max}DC \tag{9}$$

2.2.4 Drive Model

In this work, using one driver model that calculates acceleration or braking demand, a Proportional-integral-differential(PID) controller is adopted according to the difference between practical vehicle speed and desired speed. Depending on these speeds, the vehicle's state is identified as accelerating, braking, or at rest.

2.2.5 Driving Cycle

The driving conditions for design optimization and control target setting are based on representative Rural driving schedules(VITO), urban dynamometer Driving Schedules(UDDS), and Highway Fuel Economy Test(HWFET) driving cycles.[15] Each driving circle has unique characteristics that influence the battery state-of-charge(SOC) and motor performance.

The rural driving schedule(VITO) has moderate speed variations and longer distances, as shown in Fig. 5(a).

The urban dynamometer driving schedule(UDDS) involves Frequent stops and accelerations with low average speeds, as shown in Fig. 5(b).

Highway Fuel Economy Test(HWFET) has a high constant speed with minimal acceleration, as shown in Fig. 5(c).

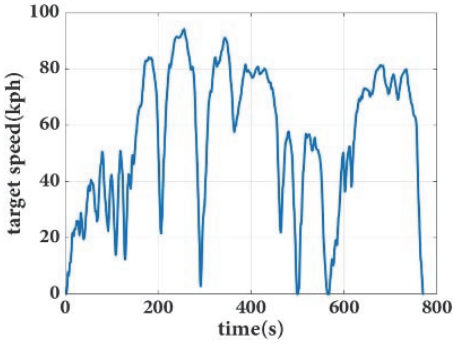

(a)

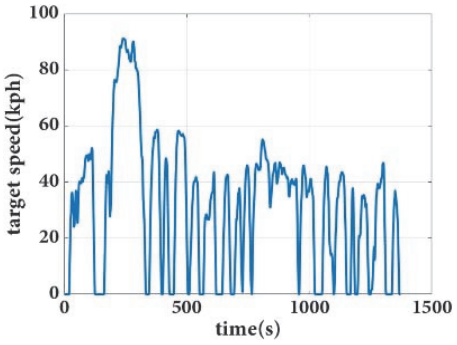

(b)

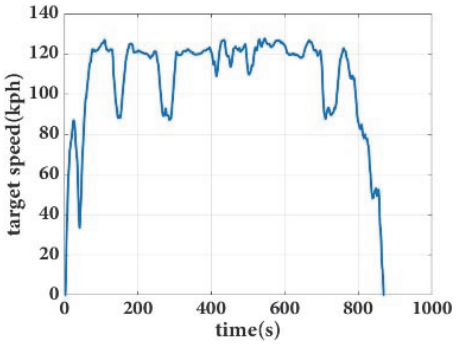

(c)

Fig. 5 Driving circles: (a) Rural driving schedule (VITO), (b) Urban dynamometer driving schedule (UDDS), (c) Highway Fuel Economy Test (HWFET)

3. Validation Simulation

To verify the reliability of the analytical model, a comparison of the actual vehicle data on AutoCar Xprime RC electric car shows the accelerations, and distance traveled using a drive cycle to test the vehicle with consideration of the maximum and minimum power of the motor with a single speed gear ratio and the battery SOC changes. Table 4(a)~(c) list the parameter references of the AutoCar Xprime RC electric car used in the validation of this simulation.

The simulation of the Autocar PrimeX RC electric car shows that the vehicle is able to chase the drive cycle up to its maximum speed of 16 km/h without any difficulty throughout the time, as shown in Fig. 6(a), (b), shows the changes of the SOC, as the initial SOC in the analysis model was set at 0.5 %, while driving the battery discharges

Table 4 RC electric car parameters references: (a) General data, (b) Motor data, (c) Battery data

(a)

General data	
Mass [kg]	6
Gravity	9.81
Drag coefficient	0.41
Downforce coefficient	1.2
Front area [m^2]	0.015
Air density [kg/m^2]	1.226
Tire radius [m]	0.0072
Rolling friction	0.015
Differential drive gear ratio	1:1
Powertrain efficiency [%]	0.92

(b)

Parameter	Value
Max torque [N · m]	67
Max speed [RPM]	2,800
Maximum efficiency [%]	92

(c)

Battery li-ion	
Capacity [A.h]	95
Power max [W]	23
Rated voltage [V]	3

gradually from 0.5 to 0.253, many times of charging of the battery can be seen due to regenerative braking. Fig. 6(c) shows the simulation result of the correct application of the motor data, where the operating points were obtained. Fig. 6(d) shows the simulation result of the acceleration and brake demand according to the speed of the vehicle by using a PID controller for the driver model. Therefore, the reliability of the model was confirmed. As the main objective of the study is the selection of the optimal gear ratio for a multi-speed transmission in EVs, the following parts present the work of the research.

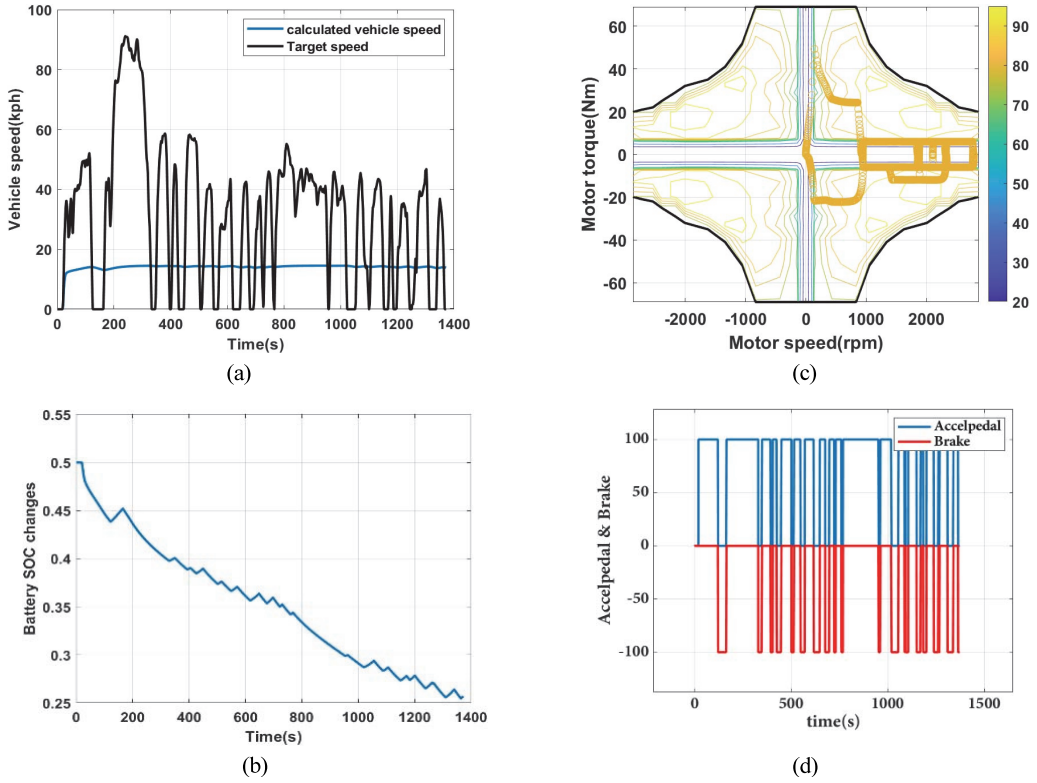

Fig. 6 Simulation results: (a) Urban dynamometer driving schedule (UDDS), (b) Battery SOC changes, (c) Motor speed-torque with operating point, (d) Acceleration and brake response from driver model adjusted by PID controller

4. Gear Ratio Selection

The gear ratio selection process in a vehicle drivetrain, particularly in electric vehicles is an important aspect of optimizing performance, efficiency, and drivability. The gear ratio determines how motor speed and torque are translated into wheel speed and torque, directly influencing acceleration, top speed, and energy efficiency. Moreover, proper gear ratio selection is a dynamic process that must adapt to changes in battery SOC to optimize performance and efficiency.

4.1 Gear Ratio Constraints

In this study, determining the gear ratio in EVs requires balancing multiple factors, including performance, efficiency, battery SOC changes, motor characteristics, and drivetrain constraints, as expressed by the following equation:

$$V_{veh} = \alpha_e \cdot 2\pi \cdot r \cdot \frac{3.6}{60 \cdot r_i \cdot N_f} \tag{10}$$

Where α_e is the motor speed, r the wheel radius, r_i the gear ratio candidates for different stages and N_f the final drive gear ratio. This equation ensures that the vehicle speed is derived based on the gear ratios and the motor speed, respecting the physical constraints of the drivetrain.

$$\mathrm{r_{i\_min}} \leq \mathrm{r_i} \leq \mathrm{r_{i\_max}} \tag{11}$$

Where r_{min} is the minimum gear ratio, r_{max} the maximum gear ratio for the given stage.

$$T_a = T_e \cdot r_i \cdot N_f \cdot \eta_{drivetrain} \tag{12}$$

Where T_a the torque at the wheel, T_e torque of the motor, and $\eta_{drivetrain}$ drive efficiency. This equation ensures that the drivetrain provide sufficient torque to meet acceleration and load requirements.

$$\eta_{total} \begin{cases} \frac{1}{\eta_{motor}} \cdot 100, if\ \eta_{motor} > 1 \\ \eta_{motor} \cdot 100 \quad if\ \eta_{motor} \leq 1 \end{cases} \tag{13}$$

This equation ensures that the motor efficiency is properly calculated and that only the feasible torque-speed region is considered for selecting a candidate gear ratio.

The selection of an optimal gear ratio must adapt dynamically depending on battery SOC constraint, to ensure efficient energy management, and allow the battery SOC stay within acceptable limits, as described in the following expressions:[16)]

$$\dot{soc}_{min} \leq \dot{soc}(k) \leq \dot{soc}_{max} \tag{14}$$

$$J_k(SOC) = \min_{r(k)} [L(r(k), \dot{soc}(k)) + J_{k+1}(\dot{soc}(k+1))] \tag{15}$$

Eq. (15) defines the dynamic programming approach using backward recursion, as $J_k(SOC)$ is the optimal cost-to-go function and $L(r(k), SOC(k))$ the immediate cost at time k, within the feasible gear option r. This setup allows for computing the optimal gear ratio selection strategy while ensuring battery SOC is maintained and the energy consumption is minimized.

Based on the dynamic programming framework defined above, the gear ratio selection strategy seeks to align motor operation with high-efficiency zones while maintaining SOC stability throughout the drive cycle. The following section details how candidate ratios are selected and analyzed for performance.

4.2 Selection Method

Selecting an optimal gear ratio ensures that the electric motor operates within its most efficient region, thereby maximizing energy conversion from electrical to mechanical output. As illustrated in Fig. 7, the motor efficiency curve typically follows a bell-shaped profile, peaking at mid-range torque and speed. Operating outside this optimal efficiency band either at low speed-high torque or high speed-low torque increases power losses and decreases system efficiency. Therefore, the transmission must be designed to maintain the motor's operation within this efficient region across various driving conditions. The gear ratio plays a critical role in achieving this by adjusting the motor's operating point relative to the wheel speed and load demand.

In this study, we employed Dynamic Programming(DP) to optimize gear ratio selection as a sequential decision-making problem, rather than solving it as an isolated, instantaneous optimization. Unlike rule-based or instantaneous selection strategies that determine the gear ratio based only

on current motor speed or torque, DP considers the entire drive cycle. This allows the algorithm to assess how a gear decision at one point in time will affect future State of Charge(SOC), motor efficiency, and overall energy consumption.

In the DP formulation, the gear ratio is treated as a control variable, and the state variables include vehicle speed, SOC, and motor operating conditions. The DP algorithm computes a cost function at each time step, which includes energy losses due to motor inefficiency, battery consumption, and penalties for rapid shifting. Using backward recursion, the algorithm calculates the optimal cost-to-go and selects gear ratios that minimize total energy usage over the full cycle, while maintaining SOC within safe limits.

Fig. 7 also integrates motor performance data into the DP structure by using a cost function derived from the motor's torque-speed efficiency map. In particular, the cost is minimized when the motor operates in high-efficiency zones, favoring gear ratios that align with those regions. This process directly links the motor's physical characteristics to the optimization model, enabling accurate and energy-conscious gear selection.

Fig. 8 shows the effect of candidate gear ratios on the motor's torque and speed, with values mapped against the vehicle's linear motion. This conversion clearly illustrates how different gear stages shift the motor's operation across the efficiency map. The horizontal axis shows the corresponding vehicle speed, and the different lines represent the motor load under various gear scenarios. From this analysis, it becomes evident that a 4-stage transmission achieves the best balance between torque coverage and motor efficiency when evaluated using the DP approach.

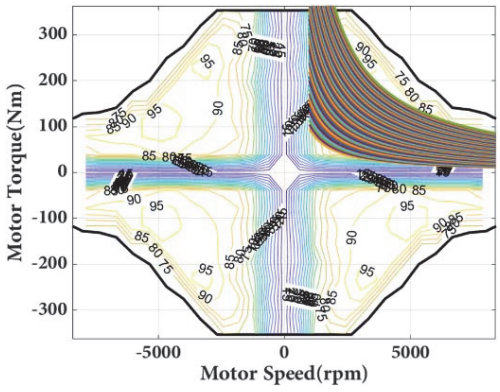

Fig. 7 Drive motor power performance and power efficiency

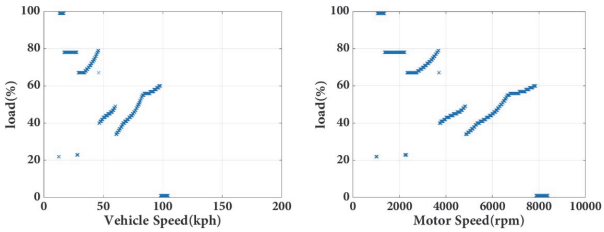

(a) (b)

Fig. 8 Impact of the Candidate Gear Selection on: (a) Motor speed, (b) Vehicle speed

Table 5 Gear ratio candidates for the selection

Gear ratio candidates			
1st stage	2nd stage	3rd stage	4th stage
10~6.7	6.7~5.0	5.0~3.0	3.0~1.5

As a result, and as summarized in Table 5, the optimal multi-stage transmission is determined to consist of four distinct gear stages, each with its own effective gear ratio range.

5. Simulation Results

As a result of analyzing the graph above, as a higher gear ratio increases torque but limits speed, a lower gear ratio increases speed but reduces torque, making acceleration and climbing difficult.

The gear ratio is set as shown in Table 6. When selecting the gear ratio at 0.3 intervals, the number of optimal gear ratio candidates is 12, 5, 7, and 6, respectively. Assuming these as reduction ratios, a total of 30 driving simulations were performed to investigate the change in battery SOC, and motor efficiency map operating point, with the results shown respectively in Table 6(a)~(d), and Figs. 9 ~ 12.

Table 6(a) provides the 1st stage gear ratios results [10.0-6.7], which shows that higher gear ratios exhibit significant SOC depletion and offer balanced performance across highway, urban, and rural driving conditions but fail to provide sufficient energy efficiency by displaying the motor operating point outside the efficient region of the motor torque-speed map and sufficient vehicle speed, as the maximum speed doesn't exceed 40 km/h, as shown in Fig. 9. This stage is suboptimal for final gear ratio selection due to its inability to balance energy efficiency and performance across all driving conditions.

Table 6 Battery SOC changes for each stage gear ratio candidates: (a) 1st stage, (b) 2nd stage, (c) 3rd stage, (d) 4th stage

(a)

1st stage gear ratio candidates	Battery SOC changes from 0.9		
	Rural way	Urban way	High way
10	0.8893	0.8851	0.8882
9.7	0.8888	0.8848	0.8878
9.4	0.8885	0.8846	0.8872
9.1	0.8880	0.8844	0.8866
8.8	0.8876	0.8842	0.8860
8.5	0.8871	0.8841	0.8852
8.2	0.8866	0.8840	0.8844
7.9	0.8860	0.8839	0.8835
7.6	0.8854	0.8836	0.8825
7.3	0.8847	0.8834	0.8814
7	0.8840	0.8830	0.8802
6.7	0.8832	0.8827	0.8832

(b)

2nd stage gear ratio candidates	Battery SOC changes from 0.9		
	Rural way	Urban way	High way
6.4	0.8824	0.8832	0.8873
6.1	0.8815	0.8831	0.8775
5.8	0.8806	0.8830	0.8734
5.5	0.8796	0.8828	0.8714
5.2	0.8780	0.8825	0.8785

(c)

3rd stage gear ratio candidates	Battery SOC changes from 0.9		
	Rural way	Urban way	High way
5	0.8767	0.8819	0.8620
4.7	0.8758	0.8815	0.8571
4.4	0.8761	0.8816	0.8535
4.1	0.8754	0.8812	0.8491
3.8	0.8754	0.8812	0.8422
3.5	0.8746	0.8811	0.8355
3.2	0.8756	0.8814	0.8210

(d)

4th stage gear ratio candidates	Battery SOC changes from 0.9		
	Rural way	Urban way	High way
3	0.8758	0.8814	0.8110
2.7	0.8758	0.8814	0.8015
2.4	0.8759	0.8815	0.8003
2.1	0.8761	0.8816	0.8012
1.8	0.8762	0.8818	0.8015
1.5	0.8759	0.8812	0.8007

In Table 6(b) and Fig. 10, the 2nd stage gear ratio [6.4-5.2] with a maximum speed of 60 km/h shows improved urban performance compared to the 1st stage. Still, it is less efficient in rural and highway conditions and fails to balance energy efficiency and SOC stability, making it unsuitable for final selection.

Table 6(c) shows that the 3rd stage gear ratio [5.0-3.2] results demonstrate a better balance across urban, rural, and highway driving conditions. Gear ratio candidate 4.4 shows strong performance in the motor operating point map, allowing the vehicle to achieve the target vehicle speed with a maximum speed of more than 120 km/h, as shown in Fig. 11. Moreover, it achieved a consistent balance between SOC stability and energy efficiency across all driving scenarios, indicating strong candidates for final gear ratio selection.

Table 6(d), and Fig. 12 show the 4th stage gear ratio candidates [3.0-1.5] results and provide the most consistent performance across all driving conditions, effectively minimizing SOC depletion while ensuring balanced energy efficiency. This stage offers the best overall performance with the optimal gear ratio candidate 1.8, which allows the simulated vehicle speed to follow the target speed and provides a better operating point for the drive motor.

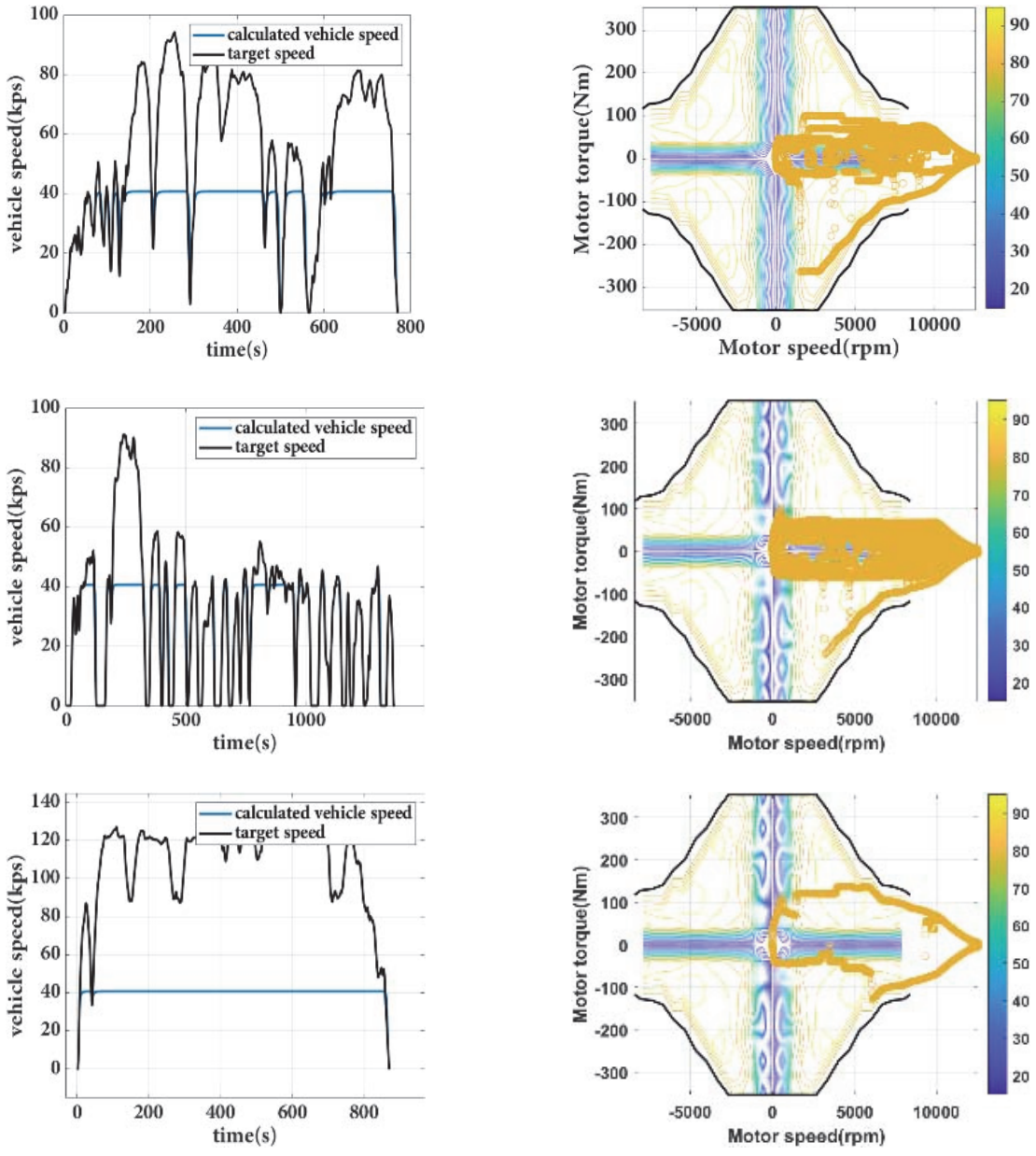

Fig. 9 Simulation Performance of each drive cycle for 1st Stage Gear Ratio Selection: (a) Simulate vehicle speed and target vehicle speed, (b) Motor operating point

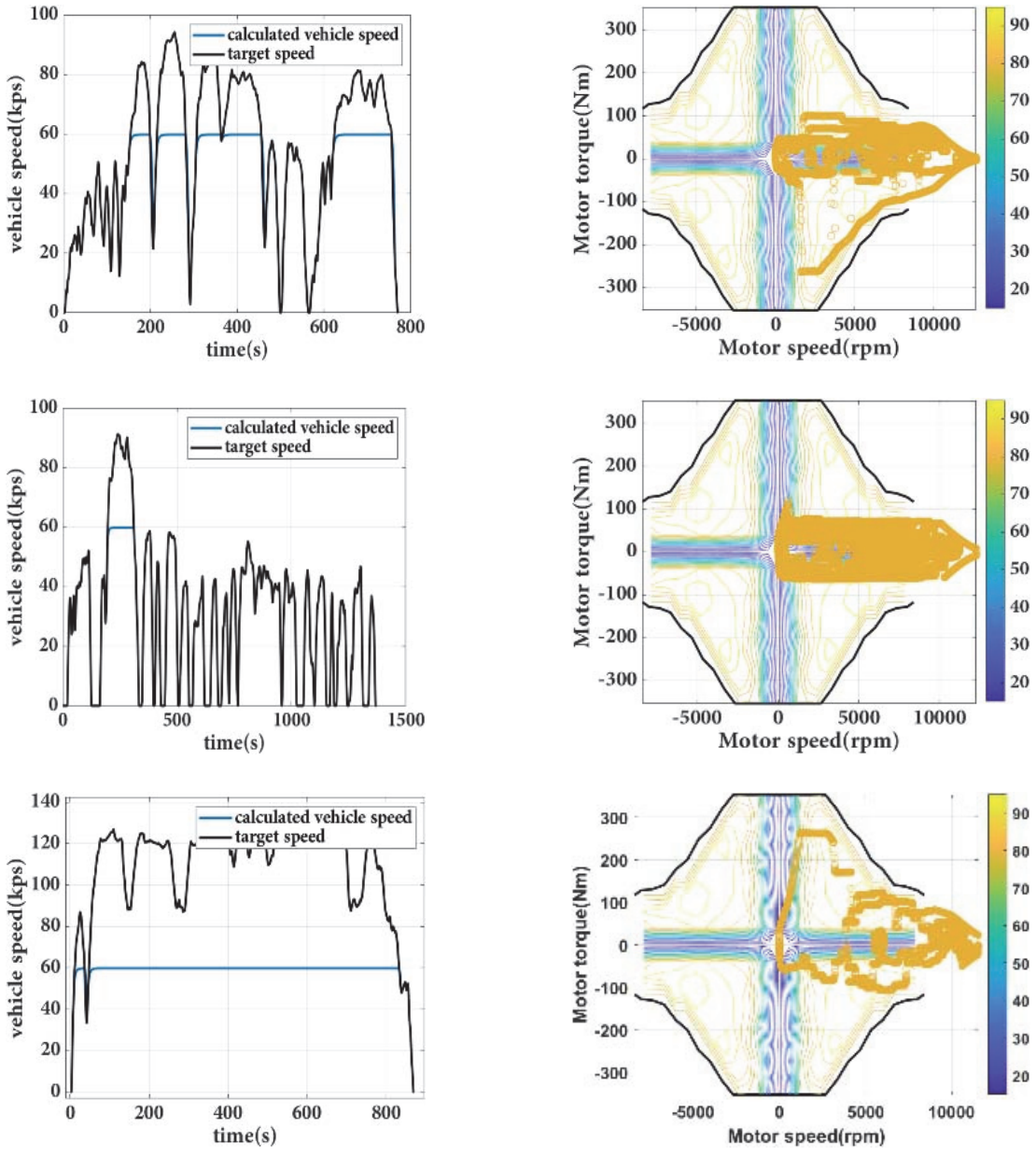

Fig. 10 Simulation Performance of each drive cycle for 2nd Stage Gear Ratio Selection: (a) Simulate vehicle speed and target vehicle speed, (b) Motor operating point

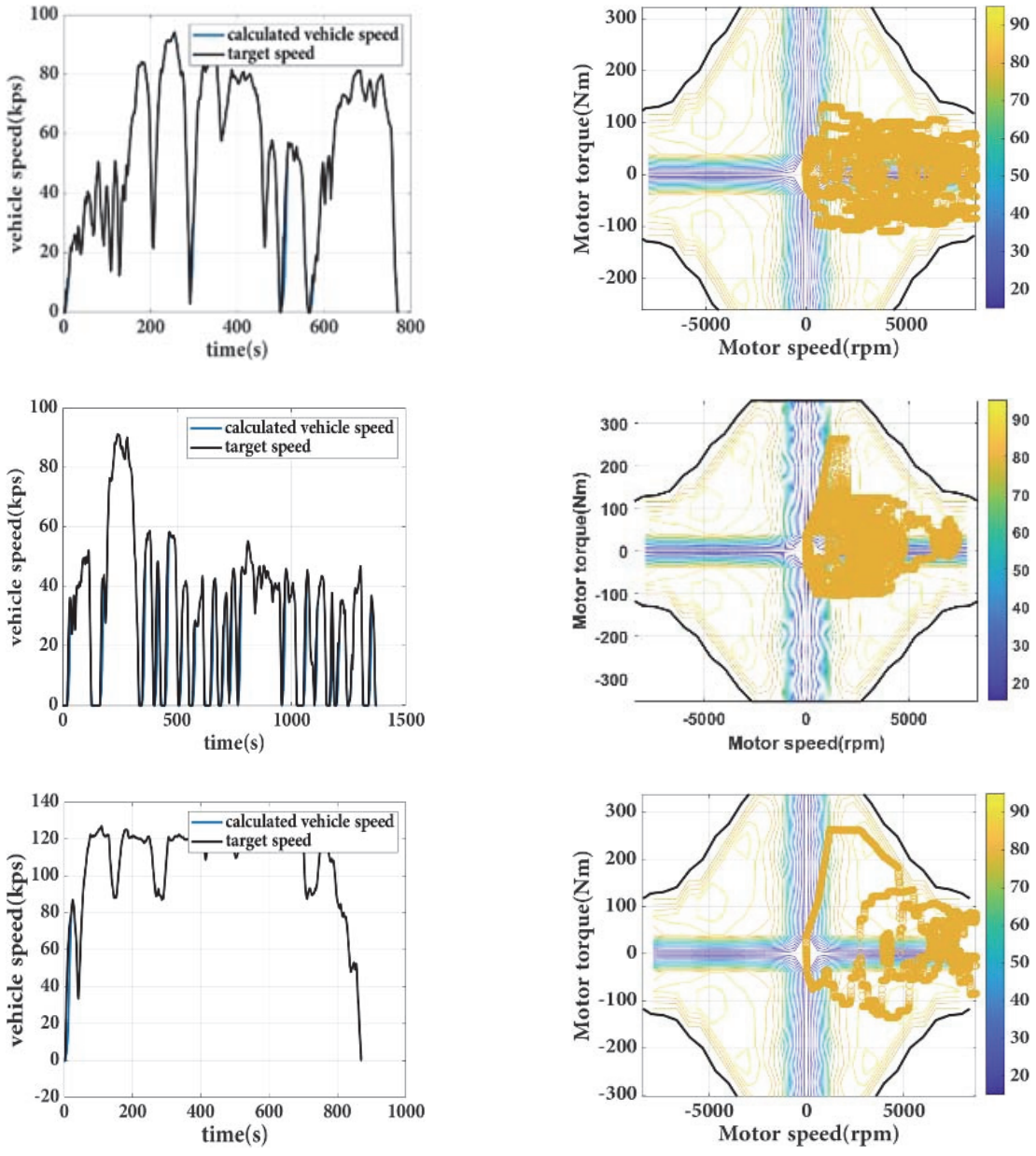

(a) (b)

Fig. 11 Simulation Performance of each drive cycle for 3rd Stage Gear Ratio Selection: (a) Simulate vehicle speed and target vehicle speed, (b) Motor operating point

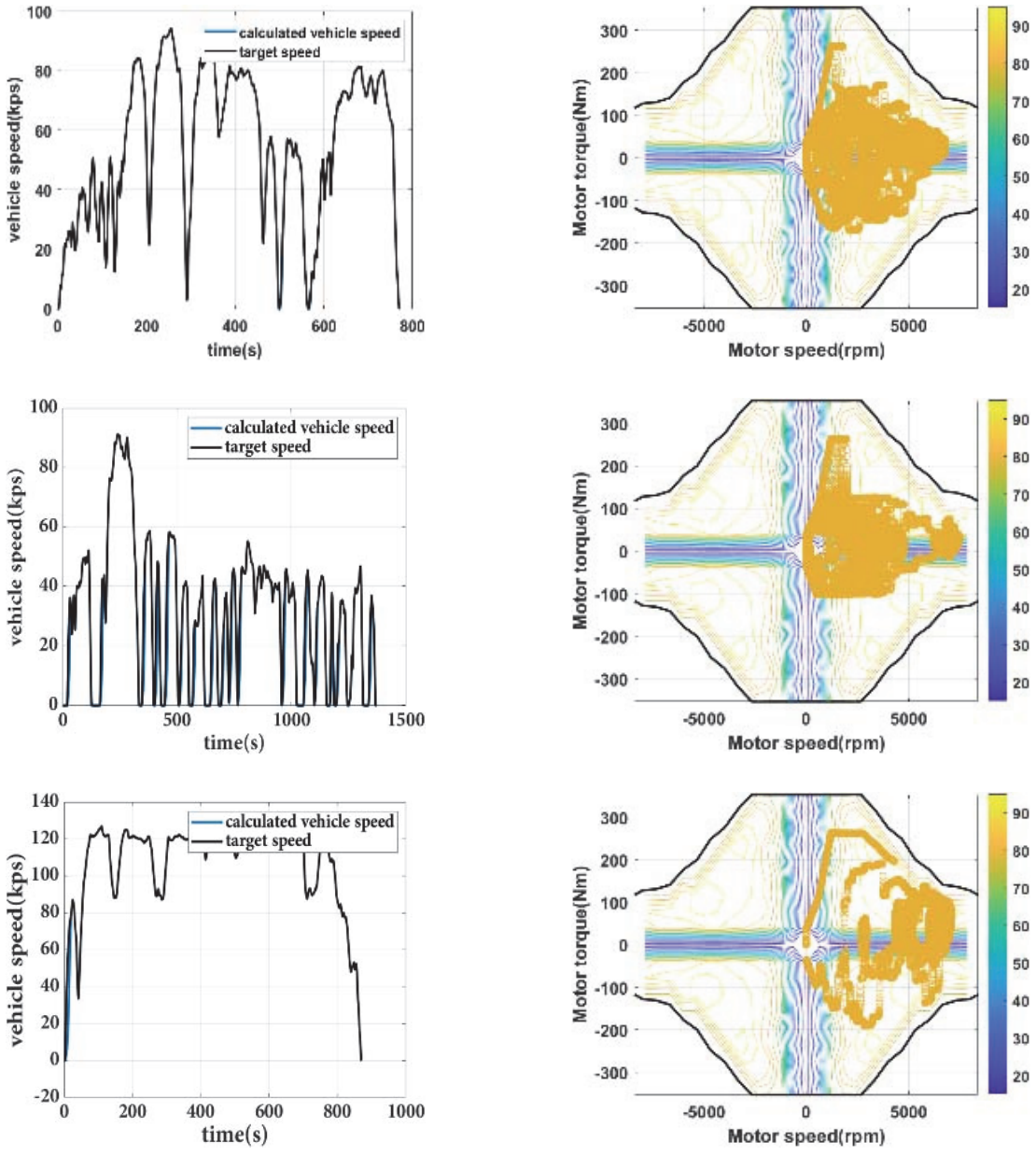

(a) (b)

Fig. 12 Simulation Performance of each drive cycle for 4th Stage Gear Ratio Selection: (a) Simulate vehicle speed and target vehicle speed, (b) Motor operating point

6. Conclusion

This study developed and optimized a simulation system for the multi-stage gear ratio transmission selection in electric vehicles, focusing on motor efficiency and battery state-of-charge(SOC) changes. Using the motor's power efficiency curve, optimal torque-speed regions were identified, and the number of gear stage ratio candidates was carefully selected to balance performance and complexity. The optimal gear ratio selection emerges from the 3rd and 4th stages respectfully with gear ratio candidates 4.4 and 1.8, where balanced energy efficiency is achieved across all driving cycle scenarios. The insights gained from this work offer valuable guidance for future electric vehicle transmission design and control systems, particularly as energy efficiency and battery longevity become increasingly critical in the transition to sustainable mobility.

Acknowledgement

This work was supported by the National Research Foundation of Korea(NRF) grant funded by the Korea government(MSIT)(No.202300180001).

References

1) A. Saha, V. Simic, T. Senapati, S. Dabic-Miletic and A. Ala, “A Dual Hesitant Fuzzy Sets-Based Methodology for Advantage Prioritization of Zero-Emission Last-Mile Delivery Solutions for Sustainable City Logistics,” IEEE Transactions on Fuzzy Systems, Vol.31, No.2, pp.407–420, 2022.
2) M. Ehsani, Y. Gao and A. Emadi, Modern Electric, Hybrid Electric, and Fuel Cell Vehicles: Fundamentals, Theory, and Design, 3rd Edn., CRC Press, Boca Raton, FL, 2018.
3) X. Zhang and C. Mi, Vehicle Power Management: Modeling, Control, and Optimization, 1st Edn., Springer, Berlin, 2011.
4) C. C. Chan and Y. S. Wong, “Electric Vehicles Charge Forward,” IEEE Power and Energy Magazine, Vol.2, No.6, pp.24–33, 2004.
5) J. R. Hendershot and T. J. E. Miller, Design of Brushless Permanent-Magnet Motors, 1st Edn., Springer, Berlin, 2010.
6) A. Emadi, Y. J. Lee and K. Rajashekara, “Power Electronics and Motor Drives in Electric, Hybrid Electric, and Plug-in Hybrid Electric Vehicles,” IEEE Trans. Industrial Electronics, Vol.55, No.6, pp.2237–2245, 2008.
7) S. M. Lukic and A. Emadi, “Effects of Drivetrain Hybridization on Fuel Economy and Dynamic Performance of Parallel Hybrid Electric Vehicles,” IEEE Trans. Vehicular Technology, Vol.53, No.2, pp.385–389, 2004.
8) S. Piller, M. Perrin and A. Jossen, “Methods for State-of-Charge Determination and Their Applications,” Journal of Power Sources, Vol.96, No.1, pp.113–120, 2001.
9) D. W. Gao, C. Mi and A. Emadi, “Modeling and Simulation of Electric and Hybrid Vehicles,” Proceedings of the IEEE, Vol.95, No.4, pp.729–745, 2007.
10) X. Hu, S. Li and H. Peng, “A Comparative Study of Equivalent Circuit Models for Li-ion Batteries,” Journal of Power Sources, Vol.198, pp.359–367, 2012.
11) A. Sciarretta and L. Guzzella, “Control of Hybrid Electric Vehicles,” IEEE Control Systems Magazine, Vol.27, No.2, pp.60–70, 2007.
12) X. Liu, J. Du, X. Cheng, Y. Zhu and J. Ma, “An Adaptive Shift Schedule Design Method for Multi-Gear AMT Electric Vehicles Based on Dynamic Programming and Fuzzy Logical Control,” Machines, Vol.11, No.9, Paper No.915, 2023.
13) L. Guzzella and A. Sciarretta, Vehicle Propulsion Systems: Introduction to Modeling and Optimization, 3rd Edn., Springer, Berlin, 2013.
14) D. G. Thomas, Fundamentals of Vehicle Dynamics, 1st Edn., Society of Automotive Engineers, 1992.
15) United States Environmental Protection Agency, “Dynamometer Drive Schedules,” [Online] Available: https://www.epa.gov/vehicle-and-fuel-emissions-testing/dynamometer-drive-schedules, 2024.
16) H. S. Yi, J. B. Jeong, S. W. Cha and C. H. Zheng, “Optimal Component Sizing of Fuel Cell-Battery Excavator Based on Workload,” International Journal of Precision Engineering and Manufacturing-Green Technology, Vol.5, No.1, pp.103–110, 2018.